

RESEARCH ARTICLE

# MISSMARPLE: Milan Small-SaMple Automated Radiocarbon Preparation LinE for atmospheric aerosol

F Crova<sup>1</sup>, F Salteri<sup>1</sup>, S Barone<sup>2,3</sup>, G Calzolari<sup>2</sup>, A Forello<sup>1,3</sup>, M Fedi<sup>2</sup>, L Liccioli<sup>2</sup>, G Valli<sup>1</sup>, R Vecchi<sup>1</sup> and V Bernardoni<sup>1</sup> 

<sup>1</sup>Department of Physics – Università degli Studi di Milano and INFN, Milan, Italy, <sup>2</sup>INFN (Istituto Nazionale di Fisica Nucleare), Sesto Fiorentino, Italy and <sup>3</sup>Department of Physics and Astronomy – Università degli Studi di Firenze, Sesto Fiorentino, Italy  
**Corresponding author:** V. Bernardoni; Email: [vera.bernardoni@unimi.it](mailto:vera.bernardoni@unimi.it)

**Received:** 16 January 2024; **Revised:** 18 June 2024; **Accepted:** 29 June 2024

**Keywords:** accelerator mass spectrometry (AMS); atmospheric aerosol; elemental carbon; radiocarbon; total carbon

## Abstract

Radiocarbon measurements on the carbonaceous aerosol fractions are an effective tool for aerosol source apportionment. For these measurements, a new sample preparation line (MISSMARPLE: Milan Small-SaMple Automated Radiocarbon Preparation LinE for atmospheric aerosol) was built in Milan (Italy). MISSMARPLE can separate different carbon fractions (i.e. total carbon (TC), elemental carbon (EC)), automates the sample combustion processes and the CO<sub>2</sub> isolation in the “combustion line”, and was designed to handle small samples, of about 50 µg carbon. The CO<sub>2</sub> obtained in the combustion line is then reduced to graphite in the graphitization line for subsequent accelerator mass spectrometry (AMS) analysis at the INFN-LABEC in Sesto Fiorentino (Italy). MISSMARPLE was tested for reproducibility of <sup>14</sup>C/<sup>12</sup>C ratio in primary standard samples, for background contamination by the analysis of blank samples (graphite with zero percent Modern Carbon (pMC)), and for accuracy by the analysis of IAEA-C7 for pMC(TC) and NIST RM8785 for pMC(EC) used as secondary standards. Measurements were carried out in different AMS runs. Reproducibility of <sup>14</sup>C/<sup>12</sup>C was within 1.2%; blank values were down to 2.2 ± 0.2 pMC in the latest AMS run, and both IAEA-C7 and NIST RM8785 measurements were within 1σ with the reference value (but for one IAEA-C7 sample within 2.3σ). These results point to MISSMARPLE as a new, valuable tool for aerosol sample preparation for radiocarbon measurements to be exploited not only on traditional 24-h samples but also when small carbon quantities are available (e.g. collected at remote sites or with high temporal resolution).

## 1. Introduction

Carbonaceous particles are among the main constituents of atmospheric aerosol with effects on human health due to the presence of carcinogenic organics and elemental carbon (Cavalli et al. 2016; WHO 2021). Further, impact on Earth radiation balance is also recognized, even though the most recent estimates of the possible positive contribution of atmospheric aerosol to the Earth radiation balance (enhancing greenhouse gases effects) performed by the Intergovernmental Panel for Climate Change (IPCC) are reduced compared to those in previous IPCC reports (IPCC 2021). In this framework, accurate source apportionment is essential for developing efficient, science-based abatement strategies targeting these particles.

<sup>14</sup>C/<sup>12</sup>C ratio measurements in the total carbon fraction of atmospheric aerosol (TC) were already identified in 1980 as a useful tool to identify fossil/non-fossil source contributions (Currie et al. 1980). Indeed, as radiocarbon half-life best estimate is 5700 ± 30 years (National Nuclear Data Center 2024), fossil fuels are so “old” that they are basically radiocarbon-free (million years are needed for their formation), whereas biogenic and biomass burning sources are characterized by a <sup>14</sup>C/<sup>12</sup>C ratio similar to the contemporaneous atmosphere. The method was widely applied in the literature, sometimes



coupling radiocarbon measurements on TC to other tracers for a more refined source apportionment (e.g. Gelencsér et al. 2007; Holden et al. 2011; Salma et al. 2017; among others).

As a step forward,  $^{14}\text{C}$  measurements on carbonaceous aerosol sub-fractions (elemental carbon—EC, organic carbon—OC) were proposed as a very powerful tool to better distinguish among modern sources (biomass burning, biogenic activity) (Szidat et al. 2006). Despite its importance, radiocarbon analysis on separated fractions of atmospheric aerosol is still performed by very few research groups in Europe (Bernardoni et al. 2013; Dusek et al. 2014, 2019; Szidat et al. 2004a; Zhang et al. 2012). This is mainly due to experimental difficulties related to small available carbon quantities (especially for EC) and to the need of developing suitable thermal protocols to be applied for the physical separation of carbonaceous fractions. Focusing on EC isolation, the works previously mentioned showed that the application of the protocols used for thermal-optical analysis is not suitable for the separation of carbonaceous fractions needed for  $^{14}\text{C}$  analysis through accelerator mass spectrometry (AMS). Further, to deal with the small available carbon quantities expected in the samples, one approach is the coupling of a thermal optical instrument (operated using suitable thermal protocols) to an accelerating machine with an ion source accepting gaseous samples (Agiros et al. 2015). This approach allows very high throughput in terms of number of analyzed samples, but it requires high investments both for the new facility and for newly dedicated personnel. As an alternative, recent advancements in graphitization procedures showed the possibility to efficiently perform the analysis of small-sized samples using a traditional source for solid targets (Fedi et al. 2020; Steier et al. 2017).

Our group has previous experiences in samples preparation for  $^{14}\text{C}$  analysis of atmospheric aerosol as well as in the AMS analysis of 50- $\mu\text{g}$  sized samples. Indeed, we previously developed a sample preparation line for radiocarbon measurements on aerosol carbonaceous fractions (Bernardoni et al. 2013; Calzolari et al. 2011), which performed very well in international intercomparison exercises (Szidat et al. 2013; Zenker et al. 2017). This preparation line operated at the INFN-LABEC (National Institute of Nuclear Physics, Laboratory for the Environment and Cultural Heritage) in Sesto Fiorentino (Italy), where the samples were analyzed by AMS exploiting a tandem accelerator accepting solid graphite samples. Nevertheless, the use of this pioneering preparation line was limited by (1) high carbon quantities needed for sample preparation ( $\sim 220 \mu\text{gC}$ ); and (2) high manpower required due to lack of automation.

Targeting more than 200  $\mu\text{gC}$  was due to the minimum quantities that were processable at the INFN-LABEC AMS setup at the time of that sample preparation line development. Later, the INFN-CHnet-LILLIPUT experiment has allowed the optimization of the graphitization and the AMS procedures to analyze smaller samples ( $\sim 50 \mu\text{gC}$ ) for cultural heritage purposes (Fedi et al. 2020). In CHnet-LILLIPUT, graphitization for the analysis of solid targets was maintained not only for the economical reason previously mentioned, but also for a technical reason: indeed, working with solid samples allows multiple measurements on the same target, with the possibility to improve counting statistics in subsequent analyses and to monitor the stability of the accelerator and of the beam transport conditions up to few days.

Stemming from these experiences, in this work we present a new sample preparation line for radiocarbon measurements on carbonaceous fractions of atmospheric aerosol: MISSMARPLE (Milan Small-SaMple Automated Radiocarbon Preparation LinE), developed in the frame of the INFN-ISPIRA (Integrazione di metodologie Sperimentali per la Ricerca sull'Aerosol carbonioso – Integration of experimental methodologies for carbonaceous aerosol research) experiment. MISSMARPLE is:

1. optimized for smaller samples compared to the INFN-LABEC aerosol preparation line: currently, 50  $\mu\text{gC}$  samples are prepared using MISSMARPLE for AMS analysis, but the preparation of even smaller samples is possible in principle;
2. characterized by a high degree of automation (through electro-valves, remote-controlled flow controller and thermoregulators), reducing the required man-power.

This paper describes the final setup of MISSMARPLE and the validation tests carried out, showing that the line is a new, valuable, and reliable tool to be exploited for  $^{14}\text{C}$  analysis in atmospheric aerosol carbon fractions. Further, first AMS results on environmental samples prepared using MISSMARPLE are shown as examples.

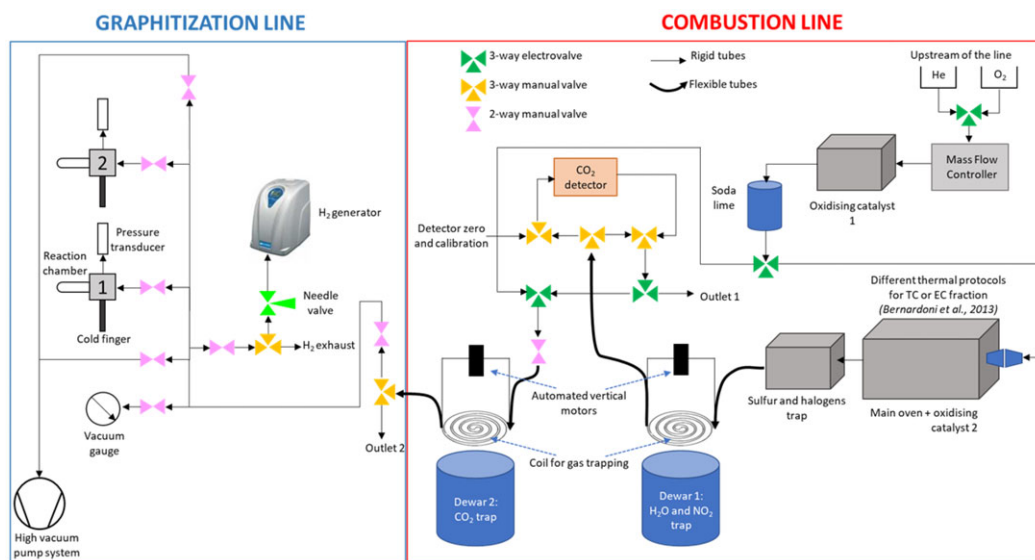


**Figure 1.** MISSMARPLE block diagram. The two main parts (the combustion line and the graphitization line) are highlighted inside the outer rectangles.

## 2. MISSMARPLE description

The block scheme of the MISSMARPLE (Figure 1) is analogous to the one of the line for aerosol sample preparation operating at INFN-LABEC (Calzolari et al. 2011) and it is structured in 4 parts:

1. Incoming gases selection and purification;
2. Sample combustion;
3. CO<sub>2</sub> purification;
4. Graphitization line.

In the following, parts 1–3 will be indicated as “combustion line”, collectively. MISSMARPLE combustion and graphitization lines are described in detail in sections 2.1 and 2.2.

To limit contaminations as much as possible, stainless-steel and quartz are the only constituents of the line, but for:

1. Kalrez 8900 O-rings (certified to have an outgassing rate less than  $2.7 \times 10^{-7}$  mbar·liter·sec<sup>-1</sup>·cm<sup>-2</sup> up to 290°C), used for the O-ring in the Swagelok Ultra-Torr vacuum fittings needed to connect quartz parts to the rest of the line and in the conic joint O-ring (see section 2.1.2);
2. electro-valves separation membrane (made in FFKM, inert and similar to Kalrez).
3. non-dispersive infrared (NDIR) detector (section 2.1.4) with a gold-coated cell.

### 2.1 Combustion line

#### 2.1.1 Incoming gases selection and purification

To isolate the carbonaceous fraction of interest for further AMS analysis, the suitable thermal protocol (involving different carrier gases and temperature steps) is applied as reported in Bernardoni et al. (2013). In MISSMARPLE, the proper gas needed during sample preparation (depending on the analyzed fraction and the combustion step) enters the line through the first electro-valve and its flowrate is remotely controlled by a mass-flow controller. The latter can manage more than one gas type thanks to

the presence of different internal calibrations remotely selected. In our case, either high-purity helium (He 5.6) or high-purity oxygen (O<sub>2</sub> 5.0) can be selected. To guarantee that every possible residual carbonaceous contamination in the carrier gas is removed before reaching the sample, the carrier gas moves through oxidizing CuO grains heated at 800°C. This ensures oxidation of any possible carbonaceous contamination to CO<sub>2</sub> and subsequent removal through a soda-lime trap.

### 2.1.2 Sample combustion

As in the INFN-LABEC line, in MISSMARPLE sample combustion is carried out in an in-house made double-oven, including a part for sample combustion (main oven) and another one to lodge the oxidizing catalyst. The core of the oven is a double quartz furnace surrounded by two heating coils that can be separately controlled. Ceramic blankets thermally separate the two furnaces to ensure independent temperature control. The main oven and the oxidizing catalyst are kept in the same box as near as possible, compatibly with independent thermal behavior, to minimize possible condensation of organics at the main oven outlet.

This double oven is smaller in MISSMARPLE than in the INFN-LABEC line, as it was re-designed for smaller samples. MISSMARPLE main oven quartz furnace has 15 mm inner diameter and 160 mm length. It can be opened thanks to a quartz conic joint, allowing the insertion of the sample through a suitable sample holder which is 40 mm long (i.e. much smaller than the 100 mm of the INFN-LABEC line as smaller samples are managed). Thus, in principle, a sample rectangular area of about 15 cm<sup>2</sup> at most can be inserted in MISSMARPLE (in the previous INFN-line the maximum sample area was about 100 cm<sup>2</sup>), but due to the circular shape of the samples maximum 8.5 cm<sup>2</sup> are generally used: hence, samples collected with low-volume samplers are suitable for preparation with MISSMARPLE. The sample holder is placed in the part of the oven where the temperature is uniform within ± 3°C. Temperature is controlled by a remote controllable thermoregulator coupled to a thermocouple. The heating coil surrounding the main oven furnace can generate up to 350 W allowing the flash-heating procedures (up to 200°C/min) needed to minimize possible sample pyrolysis (especially when EC isolation has to be performed). Due to the small size of the furnace, this power ensures flash-heating despite the weak thermal insulation needed for a relatively rapid cooling after sample combustion (< 45 minutes to cool down to 70°C). The second part of the quartz furnace (internal diameter: 10 mm, length: 160 mm) is filled with CuO oxidizer to ensure that all combustion products reach the maximum oxidizing status.

### 2.1.3 CO<sub>2</sub> purification

CO<sub>2</sub> must be isolated from all the other combustion products (indeed, aerosol may contain several components, besides carbonaceous ones) and from carrier gases before graphitization. To this aim, the carrier gas drives the combustion gases through two chemical traps for halogens and sulfur oxides (reagents: EA-1000 and Silver Vanadate from Perkin Elmer). Then, remaining gases flow through two cold traps aiming at H<sub>2</sub>O&NO<sub>2</sub> removal for final CO<sub>2</sub> isolation, and subsequent CO<sub>2</sub> trapping. The cold traps exploit the temperature gradient created in a dewar partially filled with liquid nitrogen. In each of these traps, the gases flow through a horizontal stainless-steel coil that can be moved vertically inside the dewar till the desired temperature is reached (see Calzolari et al. 2011 for details). Compared to the INFN-LABEC line, in MISSMARPLE each coil is connected to the rest of the line through flexible stainless-steel tubes, and its positioning inside the dewar is performed using a vertical stepper motor automatically and continuously controlled by the software to maintain the temperature chosen for H<sub>2</sub>O&NO<sub>2</sub> trapping (−60°C ± 2°C) and for CO<sub>2</sub> trapping (−145°C ± 5°C) (Calzolari et al. 2011) thanks to a feedback loop exploiting the reading of a PT100 probe. The temperature profile inside the dewars is shown in Figure 2 and it depends on the trap as the dewars are different due to the operational temperature ranges needed, requiring different temperature gradients. More in detail, the height of the

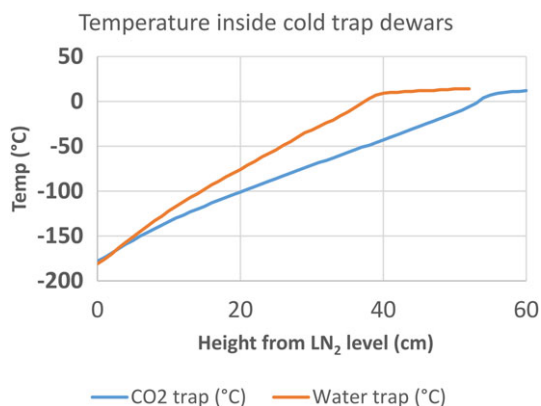


**Figure 2.** Temperature profile inside the cold trap dewars.

dewars is 50 cm for the H<sub>2</sub>O&NO<sub>2</sub> trap (dewar KWG 32 C) and 65 cm for the CO<sub>2</sub> trap (dewar KWG 34 C). It is noteworthy that in both cases, the temperature range of interest lies in about 3 cm.

Once the sample combustion is finished, the CO<sub>2</sub> trap coil is flushed with helium through a fast line bypassing the upstream main oven and traps. Then, the coil is isolated from upstream, cooled down to liquid nitrogen temperature, and then connected to the graphitization line (previously suitably prepared as described in section 2.2) using manual valves upstream and downstream of the CO<sub>2</sub> trap.

#### 2.1.4 CO<sub>2</sub> detector

In the path between the H<sub>2</sub>O and the CO<sub>2</sub> cold trap, a non-dispersive infrared detector (NDIR) was placed to monitor the complete CO<sub>2</sub> evolution during combustion steps. It is noteworthy that only CO<sub>2</sub> and the carrier gas are present in the line after the H<sub>2</sub>O trap. Thus, the detector is expected to respond to CO<sub>2</sub> concentration only, as no absorption by the carrier gases is present in its detection range.

#### 2.1.5 Details on combustion line automation

MISSMARPLE combustion line operation during sample preparation is fully automated and it is controlled by a software developed in-house using LabVIEW. The software allows to apply suitable thermal protocols (carrier gas, time length, and temperature of the steps) and to control cold-traps. Automation exploits the following elements, remotely controlled:

1. Electro-valves: 3-way electro-valves were used (stainless-steel body and FFKM separation membrane). They can be controlled by the software through a solid-state relay module in a National Instruments Data Acquisition System (DaQ);
2. digital, remote controllable, mass-flow controller (0–200 cc/min);
3. linear translation stages for cold-trap positioning, which are controlled exploiting PT100 measurements performed by a PT100-reading module in the DaQ;
4. Thermoregulators (K-type thermocouples are used for oven temperature readings).

## 2.2 Graphitization line

MISSMARPLE graphitization line is based on the implementations carried out in the INFN CHnet-LILLIPUT experiment (details in Fedi et al. 2020). It aimed at dealing with the graphitization of samples smaller than those traditionally managed in the LABEC sample preparation lines (Calzolari et al. 2011; Fedi et al. 2007, 2013). Briefly, CO<sub>2</sub> reaction with hydrogen at high temperature through an iron catalyst

is exploited for graphitization (Bosch reaction) (Vogel et al. 1984). To limit losses during the insertion of the iron + graphite into the sample holders for AMS analysis, iron is pressed into a suitable copper insert before graphitization (Steier et al. 2017). Further, the graphitization chamber volume (about 1.5 cm<sup>3</sup>) was reduced compared to traditional lines to maintain a high graphitization efficiency.

Before transferring the CO<sub>2</sub> from the combustion line to the graphitization line, the iron catalyst is purified in two subsequent heating steps:

1. 600°C in vacuum (lower than 10<sup>-3</sup> mbar) for 30 minutes
2. 350°C in 800 mbar of H<sub>2</sub> for further 30 minutes.

At the end of the iron purification, the line is evacuated from H<sub>2</sub> (lower than 8·10<sup>-4</sup> mbar). Then the coil containing residual He and the CO<sub>2</sub> from the sample combustion (already cooled to liquid nitrogen temperature) is connected to the graphitization line. All the He is then evacuated (lower than 8·10<sup>-4</sup> mbar) and—after isolation of the system from the vacuum pump—the CO<sub>2</sub> is cryogenically transferred to the graphitization chamber, where the pressure corresponding to about 50 µgC (100 ± 5 mbar are measured thanks to a pressure transducer suitably calibrated) and H<sub>2</sub> is then added for the Bosch reaction. The tube containing the copper insert with iron is heated up to 600°C while the silver cold finger is cooled by a Peltier cooler for water vapor removal (−15°C during operation). Graphitization procedure through the Bosch reaction is generally concluded in less than 45 minutes.

The copper inserts with the graphitized samples are inserted in suitable cathodes which are analyzed by AMS at the INFN-LABEC facility thanks to a 3MV Tandem accelerator using the setup and following the procedures described in Fedi et al. (2020). The output of the analysis is expressed in terms of percent Modern Carbon (pMC) (Stuiver and Polach 1977).

### 3. Results and discussion

In the following, we report the results of the tests carried out on MISSMARPLE in terms of:

1. reproducibility of the <sup>14</sup>C/<sup>12</sup>C ratio measured on different cathodes analyzed in the same AMS run and prepared from NIST 4990C Oxalic Acid standard (in the following referred to as OxAII), in our case used as primary standard for pMC determination (section 3.1);
2. blank values in terms of pMC measured in cathodes prepared from Alfa Aesar fossil graphite (cod. 14734.TA) where pMC = 0 is expected (section 3.2);
3. accuracy through the pMC measured on cathodes prepared from secondary standards (section 3.3):
  - IAEA-C7 oxalic acid standard (reference value: pMC = 49.53 ± 0.12);
  - NIST RM8785 particulate matter. It is a particulate matter standard (certified for other chemical characteristics) already used in a previous intercomparison exercise of <sup>14</sup>C measurements on aerosol samples (Szidat et al. 2013). The intercomparison showed high interlaboratory variability for <sup>14</sup>C(TC) measurements: pMC<sub>RM8785</sub>(TC) = 43.8 ± 4.9 is reported in Szidat et al. (2013); further, some concerns about the representativeness of its thermal behavior during EC separation with respect to other environmental samples were raised. Nevertheless, neither other reference materials for these measurements nor consensus on sample treatment exist for pMC(EC) measurements. Thus, unless another intercomparison exercise is carried out, the analysis of NIST RM8785 is the only choice for a single laboratory to perform any pMC(EC) measurement validation. Best value and interlaboratory uncertainty are reported in Szidat et al. (2013): pMC<sub>RM8785</sub>(EC) = 16.0 ± 3.6.
4. CO<sub>2</sub> transfer from the combustion line to the graphitization line (section 3.4).

The results presented in the following refer to three different AMS measurement runs, which are separately discussed.

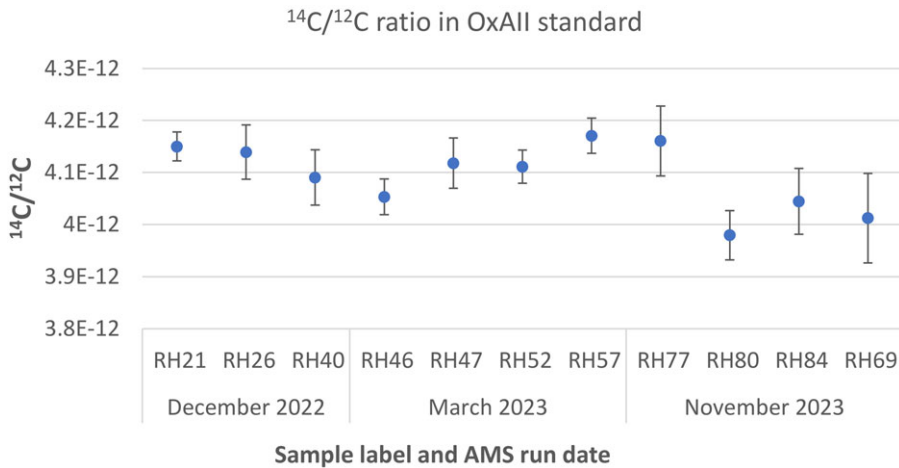


**Figure 3.**  $^{14}\text{C}/^{12}\text{C}$  ratio for the OxAll samples. Different AMS runs are separated by the grey vertical line. Error bars refer to the standard deviation of the average  $^{14}\text{C}/^{12}\text{C}$  ratio in the different batches of the same AMS run. Please note that y-axis is zoomed on the interval of interest.

### 3.1 $^{14}\text{C}/^{12}\text{C}$ reproducibility

In Figure 3, results for the  $^{14}\text{C}/^{12}\text{C}$  ratio determined on OxAll cathodes of about 50  $\mu\text{gC}$  prepared with MISSMARPLE are reported. They refer to different AMS runs which are separated by vertical lines. It is noteworthy that the values measured in different runs are not directly comparable as  $^{14}\text{C}/^{12}\text{C}$  ratio depends on the machine setting. Measurements on the same cathode prepared from OxAll standard (see labels on Figure 3 x-axis) were performed through multiple repetitions (or batches). For each sample, error bars correspond to the standard deviation of the average calculated over the repetitions on the same cathode. This relative uncertainty (evaluated in respect to each sample average value) was always within 2%. This value is higher than the one generally found using the INFN-LABEC line, but this can be easily understood considering that the sample analyzed here are more than 4-times smaller than those prepared in the past. So, poorer counting statistics is expected due to the lower extracted currents. Minor variabilities in the uncertainties associated to different cathodes (see Figure 3) can be understood considering that the final mass of the analyzed samples is estimated from the  $\text{CO}_2$  pressure in the graphitization reactor, but some differences in the final graphitized masses may arise from slight variability of the efficiency of the graphitization reaction, impacting the extraction in the source.

Reproducibility (in terms of standard deviation of the average  $^{14}\text{C}/^{12}\text{C}$  ratio measured on different OxAll cathodes analyzed in the same AMS run compared to the average) is always better than 1.2%: this is coherent with the statistical uncertainty related to the  $^{14}\text{C}$  counts available for 50- $\mu\text{gC}$  samples.

### 3.2 Background contamination by fossil graphite measurements

Background contamination of the whole preparation procedure in terms of pMC is evaluated analyzing cathodes prepared from fossil graphite (blank samples) using MISSMARPLE. Also in this case, the size is  $\sim 50 \mu\text{gC}$ .

As shown in Figure 4, relative uncertainty for the single blank cathode (i.e. standard deviation of the average for the different AMS batches) is in the range 0.15–0.87 pMC, but blank values spanned in the range 1.8–5.2 pMC. Standard deviation of the different blanks within the same AMS run is in the range 0.3–1.6 pMC. Uncertainty associated to blank measurements impacts on the precision of the pMC determination of all other samples due to the need of blank correction, especially when low-pMC

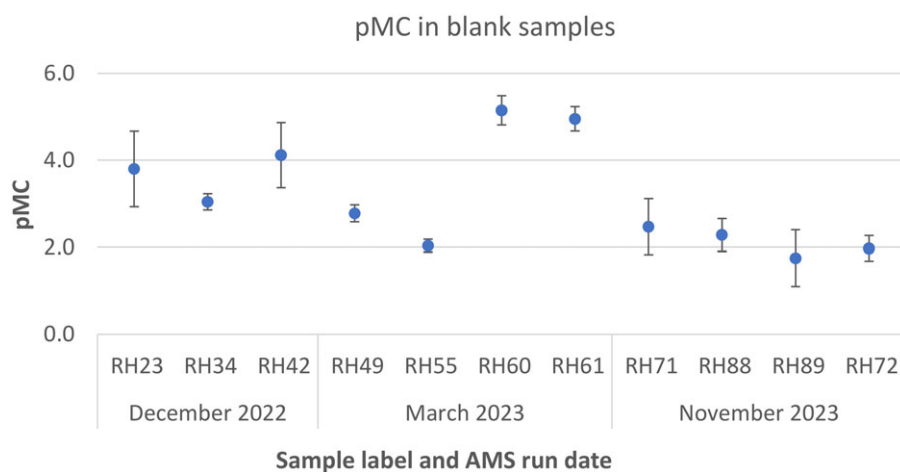


**Figure 4.** *pMC* measurements of blank samples. Different AMS runs are separated by the grey vertical line. Error bars refer to the standard deviation of the average *pMC* in the different batches of the same AMS run.

samples are present (higher relative uncertainty is expected in that case); nevertheless, all the measured blank levels and associated uncertainties are acceptable for environmental applications.

It is also important to highlight that blank values are lower and show the lowest standard deviation (0.3 pMC) in the last AMS run—indicating that improvements in the preparation procedures (e.g. performing the whole sample treatment—including weighing—in the same room, careful cleaning of the surfaces and materials for preparation before and after each sample manipulation) were effective in reducing contaminations and making blank analyses more reproducible.

### 3.3 Evaluation of measurement accuracy

#### 3.3.1 Results from IAEA-C7 samples

In each AMS run, at least one cathode prepared using the IAEA-C7 standard was measured. Blank-corrected IAEA-C7 pMC values are shown in Figure 5. Relative uncertainties were in the range 1-3% and blank-corrected values were comparable to the certified values well within 1 standard deviation for all samples but one (2.3 standard deviations).

This result confirms that our sample handling and blank correction guarantee robust measurements for pMC(TC) determination. Further, it excludes possible significant fossil contamination during sample preparation that cannot be spotted from blank measurements only.

#### 3.3.2 Results from NIST RM8785 sample preparation and measurements

Cathodes from the standard NIST RM8785 were prepared using procedures to allow the analysis of both pMC(TC) and pMC(EC). The results were blank-corrected considering the average blank values available in the same AMS run. As no filter blank was available, pMC(TC) is compared to the NIST RM8785 uncorrected values reported in Szidat et al. (2013) (see Figure 6a): both our measurements are within the 1 standard deviation range reported in the paper. However, due to the high interlaboratory variability found in Szidat et al. (2013) for NIST RM8785, the measurements presented in section 3.3.1 are a much stronger tool for the validation of the pMC(TC) measurements.

More interestingly, Figure 6b reports our pMC(EC) result compared to the ones presented by Szidat et al. (2013). Our measurement agrees within 1 standard deviation with the best estimate obtained in the



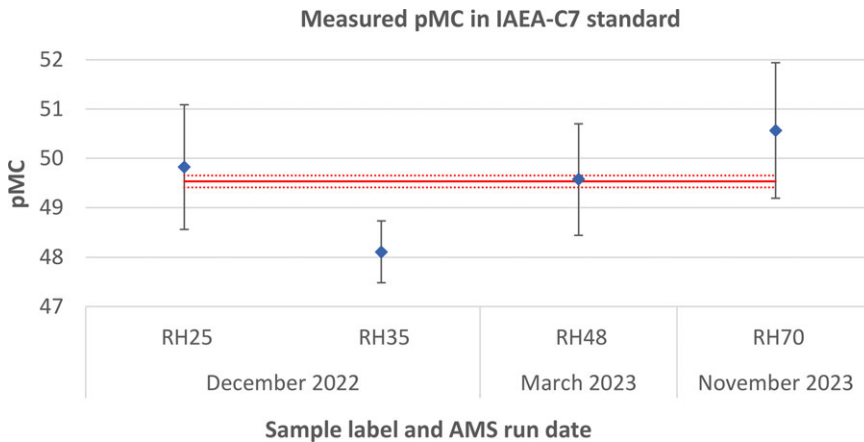


**Figure 5.** *pMC* measurements of blank-corrected IAEA-C7 samples (blue squares), and certified *pMC* value for IAEA-C7 (continuous red line represents best value, dotted red lines delimitate  $\pm 1\sigma$  range). Different AMS runs are separated by the grey vertical line. Error bars for each sample consider (root squared sum) the standard deviation of the average blank-corrected *pMC* in the different batches and the standard deviation of the average of the *pMC* of blanks in the same AMS run. Please note that y-axis is zoomed on the interval of interest.

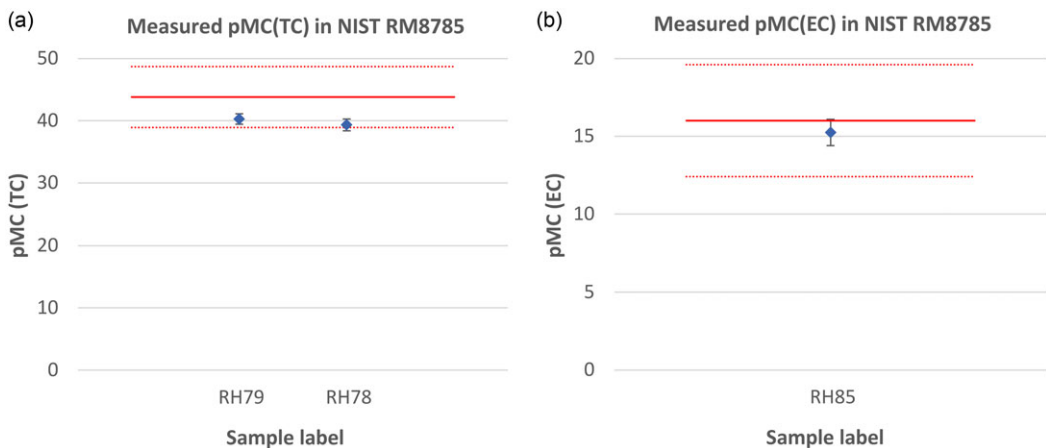


**Figure 6.** (a) *pMC*(TC) and (b) *pMC*(EC) measured on NIST RM8785. *pMC* values reported in Szidat et al. (2013) are considered as reference (continuous red line represents best value for each carbon fraction, dotted red lines delimitate the correspondent  $\pm 1\sigma$  range).

intercomparison. As previously mentioned, this is the only validation currently possible for our *pMC*(EC) measurements.

### 3.4 CO<sub>2</sub> transport to the graphitization line

The presence of a CO<sub>2</sub> detector in the combustion line (section 2.1.4) and the manometric measurements of the CO<sub>2</sub> in the combustion line were compared to ensure lack of significant losses in the process. Tests were carried out with different carbon quantities. Results are shown in Figure 7, where  $R^2 = 0.92$

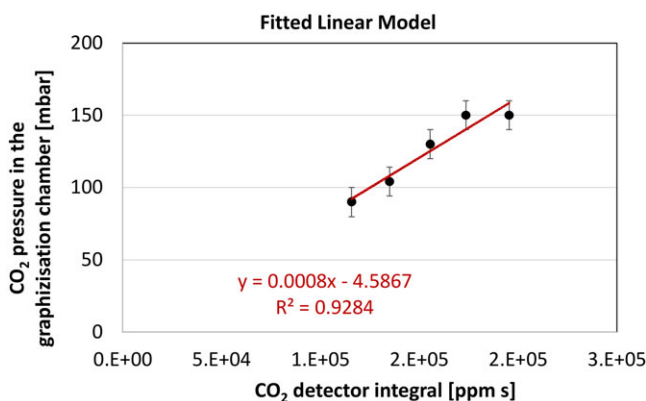


**Figure 7.** Comparison between the integral signal of the NDIR detector in the combustion line and the CO<sub>2</sub> pressure in the graphitization chamber.

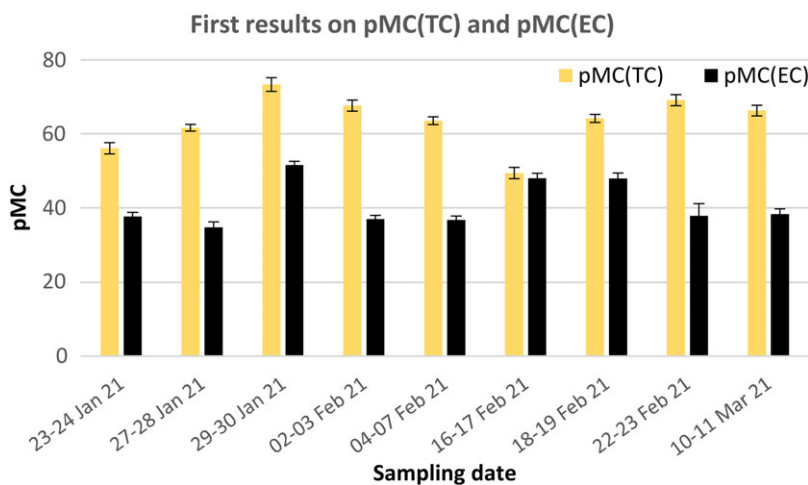


**Figure 8.** First results obtained on environmental samples by preparation using MISSMARPLE and AMS analysis at INFN-LABEC.

and the intercept of the regression line is comparable to zero. This supports the efficacy of the CO<sub>2</sub> trap in the combustion line and the CO<sub>2</sub> transfer to the graphitization line.

#### 4. First measurements on environmental samples

As an example, the first measurements of cathodes obtained preparing environmental samples using MISSMARPLE and analyzed at the INFN-LABEC AMS facility are shown in the Figure 8 and summarized here. The results refer to PM<sub>1</sub> samples collected in Bologna (Po Valley, Northern Italy) at an urban background site in January–March 2021, where also the PRIN2017 RHAPS sampling campaign was performed (Costabile et al. 2022), during a period of partial lockdown due to COVID-19 pandemic. Forty-eight-hour sampling at 2.3 m<sup>3</sup>/h on 47 mm quartz fiber filters was carried out, generally ensuring enough material for <sup>14</sup>C analysis on both TC and EC. The thermal protocols used for carbonaceous fractions isolation is the one reported in Bernardoni et al. (2013). In the analyzed samples, the average pMC(TC) is 63.5 (range 49.4–73.4) and the average pMC(EC) is 41.1 (range 34.8–51.5). The values for TC are comparable to those reported in the past for Po Valley samples (e.g. Bernardoni

et al. 2013 where PM10 samples were analyzed); the values for EC are significantly higher than the few reported for 2010 in the Po Valley (pMC range: 9–23; Bernardoni et al. 2013), but they are comparable to two values available for winter 2018 (pMC range: 41–46, Mousavi et al. 2019) and it is consistent with an increasing trend for pMC(EC) in the last years that has been recently observed also elsewhere in Europe (Crova et al. 2023). This trend can be explained considering the increasing use of diesel anti-particulate filters reducing particulate exhaust from cars (Regulation (EC) 595/2009; Damayanti et al. 2019), and to an increased use of wood burning for domestic heating and of other biofuel combustion.

## 5. Summary and perspectives

A new aerosol sample preparation facility for radiocarbon measurements on separated carbon fractions of atmospheric aerosol (MISSMARPLE) was realized in Milan (Italy) and tested. The line is targeted to small samples of 50  $\mu\text{gC}$  and it implements new technical solutions for automated sample combustion and  $\text{CO}_2$  isolation.

AMS measurements showed good performances of the line in terms of reproducibility and accuracy of the results; furthermore, background contamination (blank) values and variability are suitable for environmental samples analysis.

Reproducibility of  $^{14}\text{C}/^{12}\text{C}$  ratio was evaluated in terms of standard deviation of the average  $^{14}\text{C}/^{12}\text{C}$  ratio measurements of the primary standard (OxAII) samples in the same AMS run. Its value (compared to the average ratio) was better than 1.2%.

Single blank samples (expected pMC=0) showed pMC=5.2 as maximum value. Blanks of the latest AMS run showed both the lowest values and standard deviation in the same measurement run, highlighting that procedures to limit contamination and increase of their reproducibility have been effective (blanks measured in the latest AMS run gave pMC =  $2.2 \pm 0.2$ ).

Accuracy of pMC(TC) and pMC(EC) measurements was evaluated using IAEA-C7 (oxalic acid) and NIST RM8785 (particulate matter deposited on filter), respectively, as secondary standards. Measurements of pMC for IAEA-C7 samples were in agreement with the certified value within  $1\sigma$  (but for one sample within  $2.3\sigma$ ). pMC(EC) on NIST RM8785 resulted within  $1\sigma$  with the best estimate reported in Szidat et al. (2013).

High linearity was found between the integral signal of the NDIR  $\text{CO}_2$  detector in the combustion line and the  $\text{CO}_2$  pressure in the graphitization line, ensuring efficacy of the  $\text{CO}_2$  trapping and transfer procedures.

Finally, we demonstrated the application of MISSMARPLE in a case study of PM1 samples collected at an urban background site in the Po Valley (northern Italy). Together, the performance of the MISSMARPLE in standards, backgrounds, and unknowns indicate that the system is ready to perform reliable measurements of ambient aerosol samples.

**Acknowledgments.** This study was funded by INFN (Istituto Nazionale di Fisica Nucleare) under the experiment ISPIRA (Integrazioni di metodologie SPerimentali per la Ricerca sull'Aerosol carbonioso) and by the Italian Ministry of the Research (MUR) under the PRIN2017-RHAPS project (grant number 2017MSN7M8).

The authors thank the mechanical workshop of the Department of Physics of the University of Milan (F. Cavaliere, E. Boria), for the realization of the copper inserts for AMS sampler holder and the participant to the PRIN2017-RHAPS project for collaboration to sampling campaign.

**Competing interests declaration.** All the authors declare they have no competing interests.

## References

- Agrios K, Salazar G, Zhang Y-L, Uglietti C, Battaglia M, Luginbühl M, Ciobanu VG, Vonwiller M and Szidat S (2015) Online coupling of pure  $\text{O}_2$  thermo-optical methods—  $^{14}\text{C}$  AMS for source apportionment of carbonaceous aerosols. *Nuclear Instruments and Methods in Physics Research, Section B: Beam Interactions with Materials and Atoms*, **361**, 288–293. doi: [10.1016/j.nimb.2015.06.008](https://doi.org/10.1016/j.nimb.2015.06.008).
- Bernardoni V, Calzolari G, Chiari M, Fedi ME, Lucarelli F, Nava S, Piazzalunga A, Riccobono F, Taccetti F, Valli G and Vecchi R (2013) Radiocarbon analysis on organic and elemental carbon in aerosol samples and source apportionment at an urban site in Northern Italy. *Journal of Aerosol Science* **56**, 88–99. doi: [10.1016/j.jaerosci.2012.06.001](https://doi.org/10.1016/j.jaerosci.2012.06.001).

- Calzolari G, Bernardoni V, Chiari M, Fedi ME, Lucarelli F, Nava S, Riccobono F, Taccetti F, Valli G and Vecchi R (2011) The new sample preparation line for radiocarbon measurements on atmospheric aerosol at LABEC. *Nuclear Instruments and Methods in Physics Research Section B: Beam Interactions with Materials and Atoms* **269**, 203–208. doi: [10.1016/j.nimb.2010.12.021](https://doi.org/10.1016/j.nimb.2010.12.021).
- Cavalli F, Alastuey A, Areskoug H, Ceburnis D, Čech J, Genberg J, Harrison RM, Jaffrezo JL, Kiss G, Laj P, Mihalopoulos N, Perez N, Quincey P, Schwarz J, Sellegri K, Spindler G, Swietlicki E, Theodosi C, Yttri KE, Aas W and Putaud JP (2016) A European aerosol phenomenology - 4: Harmonized concentrations of carbonaceous aerosol at 10 regional background sites across Europe. *Atmospheric Environment* **144**, 133–145. doi: [10.1016/j.atmosenv.2016.07.050](https://doi.org/10.1016/j.atmosenv.2016.07.050).
- Costabile F, Decesari S, Vecchi R, Lucarelli F, Curci G, Massabò D, Rinaldi M, Gualtieri M, Corsini E, Menegola E, et al. (2022) On the redox-activity and health-effects of atmospheric primary and secondary aerosol: Phenomenology. *Atmosphere* **13**, 704. doi: [10.3390/atmos13050704](https://doi.org/10.3390/atmos13050704).
- Crova F, Strähl J, Jiang F and Szidat S (2023) Evolution of fossil and non-fossil emission sources of carbonaceous aerosol at a Swiss urban site from 2012 to 2020. *EAC2023, European Aerosol Conference*, Session 10-A1, Malaga (Spain), 3-8/09/2023.
- Currie LA, Klouda GA and Cooper JA (1980) Mini-radiocarbon measurements, chemical selectivity, and the impact of man on environmental pollution and climate. *Radiocarbon* **22**, 349–362.
- Damayanti S, Harrison RM, Pope F and Beddows DCS (2019) Limited impact of diesel particle filters on road traffic emissions of ultrafine particles. *Environment International* **174**, 107888. doi: [10.1016/j.envint.2023.107888](https://doi.org/10.1016/j.envint.2023.107888).
- Dusek U, Cosijn M, Ni H, Huang R-J, Meijer H and van Heuven S (2019) Technical Note: An Automated System for Separate Combustion of Elemental and Organic Carbon for  $^{14}\text{C}$  Analysis of Carbonaceous Aerosol. *Aerosol and Air Quality Research* **19**, 2604. doi: [10.4209/aaqr.2019.06.0287](https://doi.org/10.4209/aaqr.2019.06.0287).
- Dusek U, Monaco M, Prokopiou M, Gongriep F, Hitznerberge R, Meijer HAJ and Röckmann T (2014) Evaluation of a two-step thermal method for separating organic and elemental carbon for radiocarbon analysis. *Atmospheric Measurement Techniques* **7**, 1943–1955. doi: [10.5194/amt-7-1943-2014](https://doi.org/10.5194/amt-7-1943-2014).
- Fedi ME, Barone S, Barile F, Liccioli L, Manetti M and Schiavulli L (2020) Towards micro-samples radiocarbon dating at INFN-LABEC, Florence. *Nuclear Instruments and Methods in Physics Research Section B: Beam Interactions with Materials and Atoms* **465**, 19–23. doi: [10.1016/j.nimb.2019.12.020](https://doi.org/10.1016/j.nimb.2019.12.020).
- Fedi ME, Bernardoni V, Caforio L, Calzolari G, Carraresi L, Manetti M, Taccetti F and Mandò PA (2013) Status of sample combustion and graphitization lines at INFN-LABEC, Florence. *Radiocarbon* **55**, 657–664. doi: [10.1017/S0033822200057817](https://doi.org/10.1017/S0033822200057817).
- Fedi ME, Cartocci A, Manetti M, Taccetti F and Mandò PA (2007) The  $^{14}\text{C}$ -AMS facility at LABEC, Florence. *Nuclear Instruments and Methods in Physics Research Section B: Beam Interactions with Materials and Atoms* **259**, 18–22. doi: [10.1016/j.nimb.2007.01.140](https://doi.org/10.1016/j.nimb.2007.01.140).
- Gelencsér A, May B, Simpson D, Sánchez-Ochoa A, Kasper-Giebl A, Puxbaum H, Caseiro A, Pio C and Legrand M (2007) Source apportionment of PM<sub>2.5</sub> organic aerosol over Europe: Primary/secondary, natural/anthropogenic, and fossil/biogenic origin. *Journal of Geophysical Research* **112**, D23S04. doi: [10.1029/2006JD008094](https://doi.org/10.1029/2006JD008094).
- Holden AS, Sullivan AP, Munchak LA, Kreidenweis SM, Schichtel BA, Malm WC and Collett JL (2011) Determining contributions of biomass burning and other sources to fine particle contemporary carbon in the western United States. *Atmospheric Environment* **45**, 1986–1993. doi: [10.1016/j.atmosenv.2011.01.021](https://doi.org/10.1016/j.atmosenv.2011.01.021).
- IPCC (2021) Climate Change 2021: The Physical Science Basis. Contribution of Working Group I to the Sixth Assessment Report of the Intergovernmental Panel on Climate Change. In Matthews TK, Maycock T, Waterfield O, Yelekçi R, Yu R and Zhou B (eds), Contribution of Working Group I to the Sixth Assessment Report of the Intergovernmental Panel on Climate Change. Cambridge: Cambridge University Press, 2391. doi: [10.1017/9781009157896](https://doi.org/10.1017/9781009157896).
- Mousavi A, Sowlat MH, Lovett C, Rauber M, Szidat S, Boffi R, Borgini A, De Marco C, Ruprecht AA and Sioutas C (2019) Source apportionment of black carbon (BC) from fossil fuel and biomass burning in metropolitan Milan, Italy. *Atmospheric Environment* **203**, 252–261. doi: [10.1016/j.atmosenv.2019.02.009](https://doi.org/10.1016/j.atmosenv.2019.02.009).
- National Nuclear Data Center (2024) <https://www.nndc.bnl.gov/ensdf>, last access: 03 May 2024.
- Regulation (EC) 595/2009 (2009) Regulation (EC) No 595/2009 of the European Parliament and of the Council of 18 June 2009 on type-approval of motor vehicles and engines with respect to emissions from heavy duty vehicles (Euro VI) and on access to vehicle repair and maintenance information and amending Regulation (EC) No 715/2007 and Directive 2007/46/EC and repealing Directives 80/1269/EEC, 2005/55/EC and 2005/78/EC. <http://data.europa.eu/eli/reg/2009/595/oj>.
- Salma I, Németh Z, Weidinger T, Maenhaut W, Claeys M, Molnár M, Major I, Ajtai T, Utry N and Bozóki Z (2017) Source apportionment of carbonaceous chemical species to fossil fuel combustion, biomass burning and biogenic emissions by a coupled radiocarbon–levoglucosan marker method. *Atmospheric Chemistry and Physics* **17**, 13767–13781. doi: [10.5194/acp-17-13767-2017](https://doi.org/10.5194/acp-17-13767-2017).
- Steier P, Liebl J, Kutschera W, Wild EM and Golser R (2017) Preparation methods of  $\mu\text{g}$  carbon samples for  $^{14}\text{C}$  measurements. *Radiocarbon* **59**, 803–814. doi: [10.1017/RDC.2016.94](https://doi.org/10.1017/RDC.2016.94).
- Stuiver M and Polach HA (1977) Discussion: Reporting of  $^{14}\text{C}$  data. *Radiocarbon* **19**, 355–363.
- Szidat S, Bench G, Bernardoni V, Calzolari G, Czimeczik CI, Derendorp L, Dusek U, Elder K, Fedi M, Genberg J, Gustafsson Ö, Kirillova E, Kondo M, McNichol AP, Perron N, Santos GM, Stenström K, Swietlicki E, Uchida M and Prévôt ASH (2013) Intercomparison of  $^{14}\text{C}$  analysis of carbonaceous aerosols: Exercise 2009. *Radiocarbon* **55**, 1496–1509. doi: [10.2458/azu\\_js\\_rc.55.16223](https://doi.org/10.2458/azu_js_rc.55.16223).

- Szidat S, Jenk TM, Gäggler HW, Synal H-A, Fisseha R, Baltensperger U, Kalberer M, Samburova V, Wacker L, Saurer M, Schwilowski M and Hajdas I (2004a) Source apportionment of aerosols by  $^{14}\text{C}$  measurements in different carbonaceous particle fractions. *Radiocarbon* **46**, 475–484. doi: [10.1017/S0033822200039783](https://doi.org/10.1017/S0033822200039783).
- Szidat S, Jenk TM, Gäggler HW, Synal H-A, Hajdas I, Bonani G and Saurer M (2004b) THEODORE, a two-step heating system for the EC/OC determination of radiocarbon ( $^{14}\text{C}$ ) in the environment. *Nuclear Instruments and Methods in Physics Research Section B: Beam Interactions with Materials and Atoms* **223–224**, 829–836. doi: [10.1016/j.nimb.2004.04.153](https://doi.org/10.1016/j.nimb.2004.04.153).
- Szidat S, Jenk TM, Synal H-A, Kalberer M, Wacker L, Hajdas I, Kasper-Giebl A and Baltensperger U (2006) Contributions of fossil fuel, biomass-burning, and biogenic emissions to carbonaceous aerosols in Zurich as traced by  $^{14}\text{C}$ . *Journal of Geophysical Research* **111**, D07206. doi: [10.1029/2005JD006590](https://doi.org/10.1029/2005JD006590).
- Vogel J, Southon J, Nelson D and Brown T (1984) Performance of catalytically condensed carbon for use in accelerator mass spectrometry. *Nuclear Instruments and Methods in Physics Research Section B: Beam Interactions with Materials and Atoms* **5**, 289–283. doi: [10.1016/0168-583X\(84\)90529-9](https://doi.org/10.1016/0168-583X(84)90529-9).
- WHO (World Health Organization) (2021) Global air quality guidelines. Particulate matter (PM 2.5 and PM 10), ozone, nitrogen dioxide, sulfur dioxide and carbon monoxide. Geneva: World Health Organization. <https://iris.who.int/bitstream/handle/10665/345329/9789240034228-eng.pdf?sequence=1>. Last access: 14/12/2023.
- Zenker K, Vonwiller M, Szidat S, Calzolari G, Giannoni M, Bernardoni V, Jedynska AD, Henzing B, Meijer HAJ, and Dusek U (2017) Evaluation and inter-comparison of oxygen-based OC-EC separation methods for radiocarbon analysis of ambient aerosol particle samples. *Atmosphere* **8**, 226. doi: [10.3390/atmos8110226](https://doi.org/10.3390/atmos8110226)
- Zhang YL, Perron N, Ciobanu VG, Zotter P, Minguillón MC, Wacker L, Prévôt ASH, Baltensperger U and Szidat S (2012) On the isolation of OC and EC and the optimal strategy of radiocarbon-based source apportionment of carbonaceous aerosols. *Atmospheric Chemistry and Physics* **12**, 10841–10856. doi: [10.5194/acp-12-10841-2012](https://doi.org/10.5194/acp-12-10841-2012).

---

**Cite this article:** Crova F, Salteri F, Barone S, Calzolari G, Forello A, Fedi M, Liccioli L, Valli G, Vecchi R, and Bernardoni V. MISSMARPLE: Milan Small-SaMple Automated Radiocarbon Preparation LinE for atmospheric aerosol. *Radiocarbon*. <https://doi.org/10.1017/RDC.2024.96>